# Validation of ice thickness estimation method using GPR data at Qaanaaq Glacier in northwest Greenland

Ken Sato[1,2] and Shin Sugiyama[1]

[1] *Institute of Low Temperature Science, Hokkaido University*

[2] *Graduate School of Environmental Science, Hokkaido University*

To predict future glacier change, it is essential to have information on subglacial topography. Since observational ice thickness data are limited, various methods have been developed to estimate ice thickness from information measurable on glacier surfaces. However, validation is required for such methods. We have been running field observations on Qaanaaq Ice Cap in northwestern Greenland (77º28'N, 69º14'W) under the projects of GRENE (2012−2016), ArCS (2016–2020) and ArCS II (2020–). In this study, we evaluate the accuracy of the ice thickness estimation method using the results of a ground penetrating radar (GPR) survey conducted at Qaanaaq Glacier (Figure 1), an outlet glacier of the ice cap, in the summer 2022.

The GPR measurement was performed from 18th July to 12th August 2022, using a GPR system (SIR-4000, 3200 MFL) manufactured by GSSI, Inc. The central frequency of the radar wave was 40 MHz. The measurement was performed along 14 survey routes, i.e. nine sections perpendicular to the ice flow direction, one long section connecting six mass balance stakes situated along the central flowline, and four additional sections along the side margins of the glacier (Sato et al., 2023) (Figure 1). The total length of the survey routes was 21 km. Assuming a wave velocity in the glacier as $1.68 \times 10^8$ m/s (Glen et al., 1975), the ice thickness was calculated from the two-way travel time of the reflected signal. The ice thickness was estimated following the method proposed by Farinotti and others (Farinotti et al., 2009). When laminar flow is assumed in a parallel-sided slab glacier model, the flow relation can be integrated and solved for the ice thickness (Glen, 1955). The ice thickness $H_{\mathrm{est}}$ at any point of the flowline can then be calculated with the equation:

$$H_{\mathrm{est}} = \sqrt[n+2]{\frac{q}{2A} \cdot \frac{n+2}{(C\rho g \sin\alpha)^n}} \qquad (1)$$

where $\rho$ (=910 kg/m$^3$) is the density of ice, $g$ (=9.81 m/s$^2$) is the gravitational acceleration, $q$ is the ice flux, $\alpha$ is the slope of the glacier surface, $A$ is the flow rate factor and $C$ is the correction factor. According to the principle of mass conservation, the mass-balance distribution should be balanced by the ice flux and the resulting surface elevation change. Assuming that the ice density $\rho$ is constant and only plane strain is occurring, the mass conservation equation for a given width $\partial x$ on the flowline takes the form:

$$\frac{\partial h}{\partial t} = \dot{b} - \frac{\partial q}{\partial x} \qquad (2)$$

where $\partial h/\partial t$ is the time rate of ice-thickness change, $\dot{b}$ is the mass balance rate at the glacier surface. The surface slope $\alpha$ along the GPR profile line a–b (Figure 1) was calculated from GPS measurements taken every 25 m. The surface elevation change and surface mass balance are taken from our field observation data (Figure 2) (Watanabe, 2023).

Ice thickness from the GPR measurements was compared with those calculated by Equation (1) along the GPR profile line a–b. The ice thickness was overestimated in the downstream area (Figure 3). The absolute mean error was 19 m. Qaanaaq Glacier flows into a valley at 4000 m from point a. Therefore, drag from the side walls affects the ice dynamics in the lower reaches, suggesting the need of the correction of the equation for the valley shape.

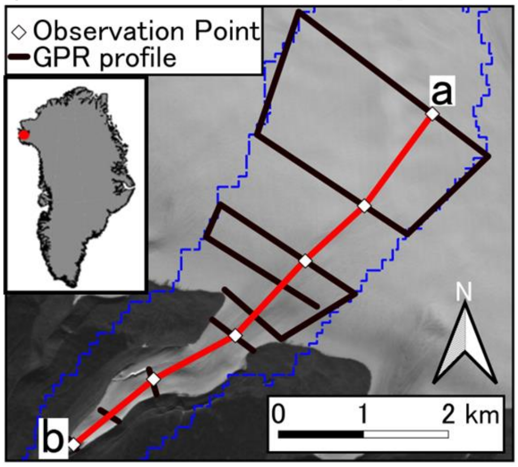


Figure 1. GPR profiles used in this study (line a-b: red) and others (black). Glacier basin boundaries (blue) and locations of the mass balance observation (diamond) are also shown. The background is a satellite image acquired in September 17, 2022

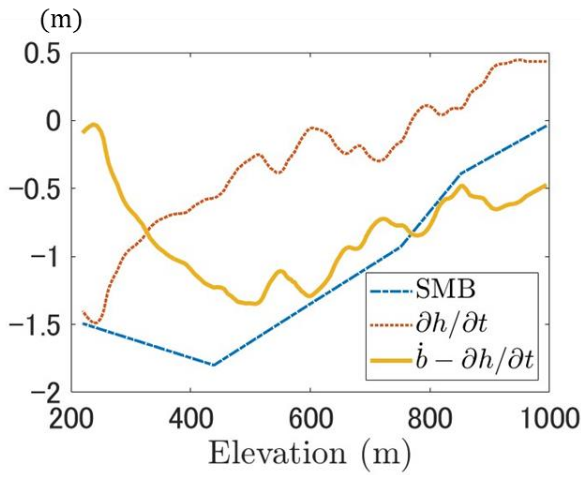


Figure 2. Surface mass balance and elevation change observed at Qaanaaq Glacier (Watanabe, 2023).

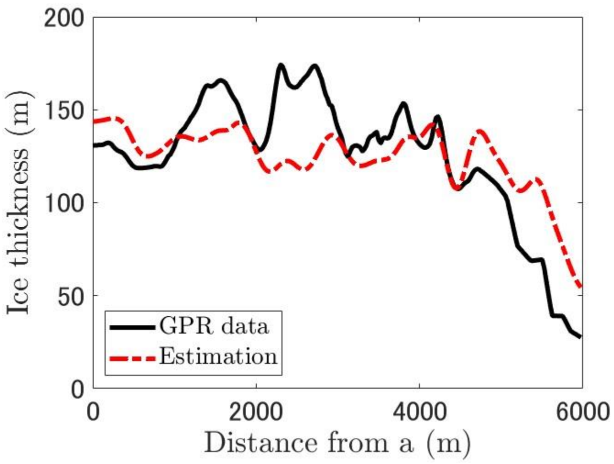


Figure 3. The ice thickness obtained from the GPR measurement along the line a-b (black) and the ice thickness estimated by Equation (1) (red).

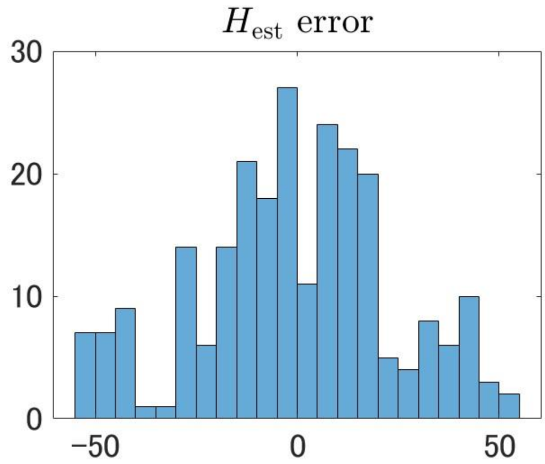


Figure 4. The error distribution of the ice thickness estimates shown in (b).

**References**


Sato, K. and S. Sugiyama, Ground penetrating radar survey on Qaanaaq Glacier in northwestern Greenland, Annual Report on Snow and Ice Studies in Hokkaido, 42, 2023.

Glen, J. and J. Paren, The Electrical Properties of Snow and Ice, Journal of Glaciology, 15, 73, 15-38, 1975.

Farinotti, D., M. Huss, A. Bauder, M. Funk, and M. Truffer, A method to estimate the ice volume and ice-thickness distribution of alpine glaciers, Journal of Glaciology, 55(191), 422-430, 2009.

Glen, J., The creep of polycrystalline ice. Proc. R. Soc. London, Ser. A, 228(1175), 519–538, 1955.

Sugiyama, S., D. Sakakibara, S. Matsuno, S. Yamaguchi, S. Matoba, and T. Aoki, Initial field observations on Qaanaaq ice cap, northwestern Greenland, Annals of Glaciology, 55(66), 25-33, 2014.

Watanabe, K., Surface mass balance of Qaanaaq Ice Cap in northwestern Greenland from 2012 to 2022, Hokkaido University, Master thesis, 2023.